Relay Stations for Electron Hole Migration in Peptides: Possibility for Formation of Three-Electron Bonds along Peptide Chains

Xiaohua Chen, Liang Zhang, Zhiping Wang, Jilai Li, Wen Wang, and Yuxiang Bu*

The Center for Modeling and Simulation Chemistry, Institute of Theoretical Chemistry, Shandong University, Jinan 250100, People's Republic of China

Received: July 4, 2008; Revised Manuscript Received: September 6, 2008

Our calculations found that the O∴O three-electron (3e) bonds (2.16∼2.27 Å) can be formed not only between two neighboring peptide units in a main chain but also between two adjacent peptide units in two different main chains in proteins. This finding may address electron hole migration from one peptide unit to the next in proteins. Evidently, stability of the O∴O 3e bonded species is strongly dependent on the component of the oligopeptides and is reduced owing to the steric hindrance of the side chains when the big chains present in oligopeptides. Besides, formation of the O∴O 3e bonds competes with the formation of the other forms of three-electron bonds depending on the component of the polypeptides. Formation of the O∴S 3e bond is thermodynamically more favorable than that of the O∴O 3e bond for the oligopeptides containing sulfur atom in their side chains. Similarly, formation of the O∴π 3e bond between aromatic ring of the side chain and the neighboring peptide unit is more stable than that of the O∴O 3e bond when the aromatic amino acids present in the oligopeptides. We infer that a series of three-electron bonds may be formed during the electron hole migration along the peptide backbone in proteins and assist electron hole transport as relay stations, supporting the peptide chain as a conduction wire. The ab initio molecular dynamics simulations of the polypeptides also support this conclusion.

Introduction

Electron hole migration along peptide backbone of proteins has become a general topic of substantial current interest, because the protein-based electron-transfer (ET) reactions play a fundamental role in a variety of biological processes.[1−7] There has been a long standing effort about the details of the electron hole transfer function of the peptide backbone in the protein-based ET reactions.[8−11] In particular, a hopping mechanism was recently proposed for such an electron hole migration along the peptide backbone[12−19] and was further supported by a subsequent molecular dynamics (MD) simulation, suggesting that the migration may proceed by changing the conformation of two neighboring peptide units.[20] This conformation change permits the carbonyl groups of the neighboring amino acids to be close enough with a O···O contact of less than 3 Å, a definite critical value, thus strongly facilitating the electron hole migration from one peptide unit to the next.[20] The iteration of this behavior leads to the electron hole migration along the peptide backbone. Further, the instantaneous coupling between the neighboring peptide bond units observed from experiments and MD simulations also validated the proposal for the peptide-based electron hole migration.[21] In addition, the charge transport in peptides is dominated by not only the components of peptide chains but also its environments.[22]

Recently, more efforts have suggested that some weakly special interactions may serve as electron transfer channels for the redox reactions in chemical and biological processes.[23−25] There are many such kinds of weak interactions in proteins which includes noncovalent and weak-covalent interactions, such as lone pair···π(1p···π) interactions,[26,27] π···π interactions,[28] cation···π interactions,[29] anion···π interactions,[30] hydrogen bonds (H-bonds),[31] and two-center, three-electron (2c-3e) bonds.[32] In a certain sense, these interactions are thought to play an important role for long-range electron transfer in proteins and for oxidative damage of cell components.[33] One of the elementary steps of the protein ET reactions is the electron hole migration along the peptide linkages, and a series of the site−site associated modes dominated by the weak interactions are formed during these migration processes as the relay stations or intermediates of protein ET reactions. It is reported that the O lone pair···π contact takes part in the ET process for the cisoid tert-butylperoxyl/phenol reactions and the two ring π···π (face-to-face) overlap allows ET from one aromatic ring to another for the tyrosyl/tyrosine reactions.[24] Our recent work has elucidated that the O···O 2c-3e bond (O∴O) may serve for the single ET channel for the radical self-exchange reaction in the peptide bond units.[25]

As far as the 2c-3e bonds are mentioned, a large body of reports have proved that the 2c-3e bonds can be encountered not only between the homogenerous atoms but also the heterogenerous atoms in many chemical and biological species, such as S∴S, N∴N, P∴P, I∴I and X∴Y (X, Y = S, O, N, P, halogen, and so forth).[34−36] The stabilization of a three-electron (3e) bond involves the interaction of a σ-bonding orbital occupied by two electrons and a σ* antibonding orbital occupied by one electron.[34,37,38] Formation of the 2c-3e bonds may considerably stabilize the corresponding complexes. In particular, the 3e bonds may instantaneously come into being and assist ET as relay stations in the chemical and biochemical processes. In 2000, Gauduel and co-workers detected the sulfur−sulfur radical anion $(RS\therefore SR^-)_{aq}$ with a 3e bond which serves as an ET intermediate before formation of the fully hydrated electrons.[39] In addition, it has been reported that the sulfur-containing compounds participate in the protein ET processes through formation of the 2c-3e bonds between the sulfur atom

* To whom correspondence should be addressed.

10.1021/jp805910x CCC: $40.75
Published on Web 10/16/2008

SCHEME 1: Schematic Representation of the Considered Dipeptide Radical Cations

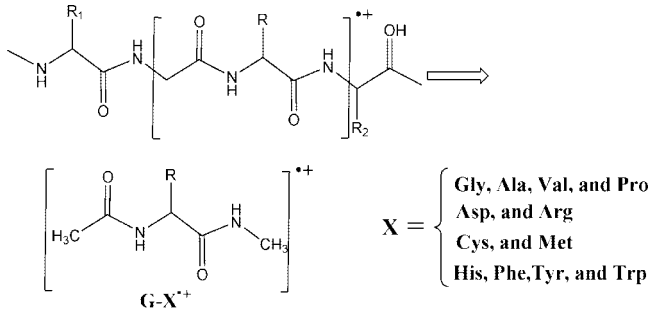

and other heteroenerous atoms, such as S, O, and N, by the intra or inter molecular interaction.[40−46] Motivated by the electron hole migration function of the sulfur-centered 3e bonds in a series of the biochemical processes and on the basis of the radical properties of the peptide bonds in proteins, we investigated the radical cations of a series of the modeled dipeptides. Interestingly, our DFT calculations have found that the 2c-3e bonds can be encountered between two O-atoms of two neighboring peptide units within the peptide chain or in two different peptide chains. The O∴O bonds, which act as the relay stations of the electron hole migration along the peptide chain, may address the charge transport from one peptide unit to the next.[20,22] Formation of the O∴O bonds competes with that of the side-chain radicals, such as indole radical of Trp (Trp$^{\bullet+}$), phenol radical of Tyr (Tyr$^{\bullet+}$), benzole radical of Phe (Phe$^{\bullet+}$), imidazole radical of His (His$^{\bullet+}$), and so on. In this case, these side-chain aromatic radicals are stabilized by the carbonyl O of the peptide bonds via forming the O$\cdots\pi$ 3e (O∴π) bonds. Therefore, a series of 3e bonds, O∴O, O∴S, O∴π or others, may be instantaneously formed to serve as relay stations for the electron hole migration in proteins and should be particularly investigated. This work offers the first comprehensive analysis about the possibility of forming the 3e bonds in proteins and their bonding characters. Exploration of such systems in general is also of interest for the understanding of the transduction of charge by polypeptide, thus interpreting charge transfer in proteins—a field of immense current interest.[22]

Theoretical Methods

To understand how electron hole migrates in proteins, two series of systems are mainly considered in the present work. For the electron hole migration, a focus problem is if the favorable residence is available for the electron hole. As mentioned above, the 2c-3e bond may be envisioned as a responsible candidate for the stabilizer of the electron hole. So, an examination is needed on a possibility of formation of the 2c-3e-bond-based electron holes between two neighboring peptide units and between two different peptide units. First, a series of dipeptide radical cations in which one of two amino acid residues is glycine[47] (Gly, see Scheme 1) were considered to be Gly-X$^{\bullet+}$ (X = Gly, Ala, Val, Asp, Arg, Cys, Met, His, Phe, Try, and Trp), forming Gly-Gly$^{\bullet+}$, Gly-Ala$^{\bullet+}$, Gly-Val$^{\bullet+}$, Gly-Asp$^{\bullet+}$, Gly-Arg$^{\bullet+}$, Gly-Cys$^{\bullet+}$, Gly-Met$^{\bullet+}$, Gly-His$^{\bullet+}$, Gly-Phe$^{\bullet+}$, Gly-Try$^{\bullet+}$, and Gly-Trp$^{\bullet+}$ dipeptides. Second, the 2c-3e bond-based electron hole between different main chains or side chains were further considered by modeling the interaction between a peptide unit and other peptide unit. Binding energies between two fragments for these systems were determined with the basic set superposition error (BSSE) correction.[48,49]

All gas-phase calculations were carried out by using Gaussian 03 suite of programs.[50] The UB3LYP[51] hybrid functional in conjunction with the 6-311+G* basis set[52] was utilized to optimize all geometries fully and to perform the harmonic vibrational analyses for confirming minima (all real frequencies) and transition state structures (one imaginary frequency). Two larger basis sets, 6-311++G(d,p) and aug-cc-pVDZ, were also used to verify the reliability of 6-311+G(d). For all dipeptides considered here, B3LYP shows essentially no dependence on a change in the size and flexibility of the basis set. In most cases, an increase in the basis set caused changes in the energy gaps between the same dipeptide isomers, but no changes in the ordering of the isomers were found. To obtain more accurate relative energies of isomers, single-point energies were recalculated for the global and local minima at the B3LYP/aug-cc-pVDZ//B3LYP/6-311+G(d)[53] level of theory. In addition, to further verify the applicability of the B3LYP/6-311+G* method, the MP2/6-311+G* method was also carried out to examine the isomers for Gly-Gly$^{\bullet+}$. The results obtained by the MP2/6-311+G* optimizations were in agreement with those by B3LYP/6-311+G* calculations (Supporting Information, Figure S1). Therefore, the density functional theory (DFT) was mainly used to investigate the polypeptide radical cations in this work. The time-dependent density functional response theory (TD-DFT)[54] calculations were performed to find out the excitation wavelength to excite an electron from a doubly occupied bonding orbital to the lowest singly occupied antibonding orbital ($\sigma\rightarrow\sigma^*$) of 2c-3e bonded complexes with the B3LYP/6-311+G(d)-optimized geometries. The restricted molecular orbital contours were used to display the orbital character. Other data including dynamics stability of 3e bonds, energies and enthalpies, frequencies of all structures, orbital characteristics, and correlations among several quantities are listed in Supporting Information. In addition, it should be noted that the energies instead of enthalpies are used in the relevant analyses.

To validate that the lowest-energy isomers for all dipeptides are real and examine the stabilities of all the three-electron bonded species, ab initio molecular dynamics (AIMD) simulations were performed with the DMol3[55] at the density functional theory (DFT) level with a DND double numerical basis set plus polarization functions for heavy elements upon the structures obtained by B3LYP/6-311+G* optimizations, as implemented in the Accelrys′ Cerius2 package.[56] The simulations of all dipeptide models were carried out in a canonical *NVT* ensemble and total simulation time is 6.0 ps with a time step of 0.2 or 1.0 fs. Temperature was kept constant (300 K) by using Massive GGM. Besides, we also carried out the AIMD simulations for a series of oligopeptides to explore electron hole migration along the peptide chains at 1000 K.[57]

Results

The peptide radical cation can be formed by transferring an electron from its close-shell system to other electron hole, which is defined as Gly-X$^{\bullet+}$. For sake of discussion, we first define the mainly similar isomers for all the dipeptide radical cations. For all aliphatic dipeptide models, there exist three major forms based on the intramolecular weak bonding: O∴O bonded conformation (Gly-X$^{\bullet+}$_O∴O), O∴N bonded conformation (Gly-X$^{\bullet+}$_O∴N), hydrogen-bonded conformations (Gly-X$^{\bullet+}$_H$_n$, n = 1, 2, $\cdots$), as shown in Scheme 2. Each conformation may certainly have several low-energy isomers according to the spatial arrangement of the side chains and only the lowest-energy isomer is presented for all the dipeptide models in this work. When a sulfur atom is present in the side chain of amino acids, other several major conformers could be formed: S∴O bonded isomers (Gly-X$^{\bullet+}$_O∴S$_n$, n = 1, 2, 3, $\cdots$) and N∴S bonded

SCHEME 2: The General Isomers for All the Dipeptide Radical Cations

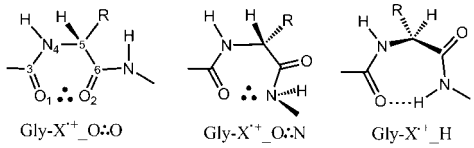

SCHEME 3: The Representative O∴π Bonded Isomers for the Dipeptide Radical Cations with Aromatic Ring in Their Side Chains

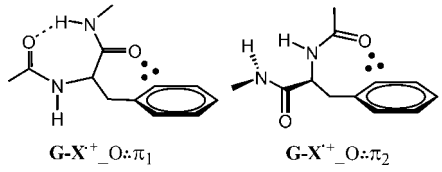

isomers (Gly-X$^{\bullet+}$_N∴S$_n$, n = 1, 2, 3,...). When an aromatic ring presents in the side chain of amino acid, such as His, Phe, Tyr, and Trp, formation of the lone-pair∴π 3e bonded conformers (Gly-X$^{\bullet+}$_O∴π_1, and Gly-X$^{\bullet+}$_O∴π_2) are possible, as displayed in Scheme 3.

3.1. Formation of O∴O 3e Bond in the Simple Dipeptide (Gly-Gly$^{\bullet+}$) Radical Cation. Gly-Gly is the simplest dipeptide without side-chains. Many possible isomers of its radical cation have been found, and only four representative isomers are shown in Figure 1 with main geometrical parameters and the relative energies with respect to the O∴O bonded isomer. The remarkable structural feature of Gly-Gly$^{\bullet+}$_O∴O is a short O···O distance (2.23 Å). Gly-Gly$^{\bullet+}$_H is 2.2 kcal/mol higher in energy than Gly-Gly$^{\bullet+}$_O∴O and marks an intramolecular H-bond between the O-atom of one peptide bond unit and the H-atom of the other (the O···H length of 2.03 Å) aligned with an elongated C−C bond (1.67 Å) between the two peptide bond units in comparison to a normal C−C bond. The Gly-Gly$^{\bullet+}$_O∴N isomer has a short O···N distance (2.39 Å) and lies 3.3 kcal/mol above Gly-Gly$^{\bullet+}$_O∴O. The last isomer, Gly-Gly$^{\bullet+}$_H$_2$, might initially have been regarded as being the most intuitively logical isomer because here the two carbonyl groups are trans and an acyl O-atom functions as a H-bond acceptor, forming a weak intramolecular H-bond of 2.05 Å to the H-atom of other peptide bond unit (Figure 1). However, Gly-Gly$^{\bullet+}$_H$_2$ is 7.8 kcal/mol higher in energy than Gly-Gly$^{\bullet+}$_O∴O and is the most unstable isomer among our considered isomers, which implies that it is difficult to come into being.[58] This analysis indicates that formation of the O∴O bonded conformer, Gly-Gly$^{\bullet+}$_O∴O, is thermodynamically favorable, being the global minimum on the potential energy surface of Gly-Gly$^{\bullet+}$.

It is noteworthy that, for Gly-Gly$^{\bullet+}$_O∴O, the O···O distance is only 2.23Å, implying a considerable bonding interaction between the O-atom pair. Further, the spin densities mainly reside on the two closely approximal O-atoms (0.47 versus 0.45), implying an electron hole to mostly localize on the two O-atoms. The singly occupied molecular orbital (SOMO), an antibonding orbital (σ*) between these two O-atoms (Figure 2), also confirms the hole localization. The second doubly occupied molecular orbital (HOMO-1, here named as DOMO) is a σ bonding one, also mainly located on these two O-atoms, as shown in Figure 2. Clearly, combination of these two MOs yields a special 2c-3e bond between these two O-atoms. In addition, a strong absorption with strong intensity (f = 0.197) in the absorption spectra of this O∴O bond with a wavelength of 436.01 nm (2.84 eV) which corresponds to a $\sigma \rightarrow \sigma^*$ transition also confirms the considerable interaction between two close O-atoms.

As a contrast to Gly-Gly$^{\bullet+}$_O∴O, we examined the trans conformers in which two carbonyl O locate on the opposite sides of peptide backbone: Gly-Gly$^{\bullet+}$_H and Gly-Gly$^{\bullet+}$_O∴N (Figure 2). For Gly-Gly$^{\bullet+}$_H, the spin densities are delocalized along the main chain of dipeptide. However, for Gly-Gly$^{\bullet+}$_O∴N, the spin densities on the approximal O and N atoms are 0.35 and 0.54. The MOs in Figure 2 indicate that there is a 2c-3e bond between the close O and N atoms arising from the interaction between the SOMO and the DOMO.[59] Actually, this O∴N 3e bond also plays a stabilization role for Gly-Gly$^{\bullet+}$_O∴N, leading to a small energy differnece of 3.3 kcal/mol over Gly-Gly$^{\bullet+}$_O∴O. These results indicate that localization of spin densities on these two close O-atoms is favorable in energy than delocalization of spin densities over the main chain and the O∴O bonded species is more stable than the O∴N bonded isomers for Gly-Gly$^{\bullet+}$.

Mechanistically, the above analyses indicate that it is thermodynamically favorable to form the O∴O bonded isomer for the Gly-Gly$^{\bullet+}$ radical cation. As a result, we deduce that the O∴O bond may be formed during electron hole migration along the peptide backbone of proteins as a relay station, which is in favor of ET from one peptide to the next in protein.[20,22]

Eventually, the question comes into being: when or in what O···O distance the 3e bond starts to form? To address this issue, potential energy surface scan was also carried out by varying the dihedral angle NCCO (D_{NCCO}) of Gly-Gly$^{\bullet+}$ ranging from the O∴O bonded isomer to an H-bonded isomer (Supporting Information, Figure S19). Figure 3 displays the dependence of the spin density distributions of Gly-Gly$^{\bullet+}$ on the dihedral angle D_{NCCO}. When D_{NCCO} is less than 30° and the distance of two O-atoms of Gly-Gly$^{\bullet+}$ is less than 3.00 Å, the spin densities mainly localize on the two O-atoms with a similar distribution. In this case, a 3e bond can be formed between the two O-atoms. When D_{NCCO} is larger than 30° and the distance of two O-atoms of Gly-Gly$^{\bullet+}$ is larger than 3.00 Å, the spin densities delocalize over the molecular framework and the symmetry of the spin density distribution on the two O-atoms is broken. So, the two O-atoms can not be linked by a 3e bond. Therefore, it is safely concluded that the O∴O 3e bond can form when the O···O distance is less than 3.00 Å in a dipeptide radical cation.

Formation of the O∴O bond in oligopeptides is also validated by examining the hexapeptide given in Supporting Information (Figure S6). Furthermore, to clarify the possibility of formation of the O∴O bonds during the protein ET processes, a series of dipeptide radical cations containing different side-chains are considered in the following statement.

3.2. Effect of Side Chains on Stability of Backbone O∴O 3e Bond. In order to investigate systematically the influence of the side chains of amino acids on the stability of the O∴O bond, alkyl groups (Ala, Val, and Pro), acidic groups (Asp), and basic groups (Arg) are considered in this section. Some common phenomena are observed for these dipeptide cation radicals: Gly-Ala$^{\bullet+}$, Gly-Val$^{\bullet+}$, Gly-Pro$^{\bullet+}$, Gly-Asp$^{\bullet+}$, and Gly-Arg$^{\bullet+}$. Similar to that in the Gly-Gly$^{\bullet+}$ case, three isomers as shown in Scheme 2, Gly-X$^{\bullet+}$_O∴O, Gly-X$^{\bullet+}$_O∴N, and Gly-X$^{\bullet+}$_H, are found for all of them. However, the O∴O bonded isomers are not the global minima but the local minima on their potential energy surfaces. The Gly-X$^{\bullet+}$_H isomers are the global minima for all of them (Table 2 and Figures S7−S10). Clearly, this observation may be attributed to the fact that all the side groups of these amino acids show the electron-donating properties and play important roles in stabilizing the radical cation when the unpaired electron is delocalized along the main chain. As a result, the relative stabilities of the three isomers for all

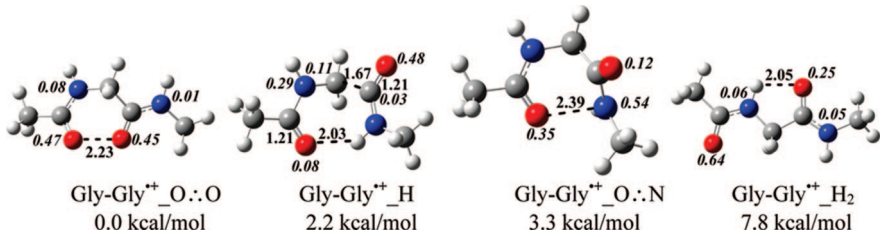

Figure 1. The major isomers of Gly-Gly$^{\bullet+}$ dipeptide with main parameters. The selected bond distances are in angstroms; the italic numbers are the atomic spin densities; and the numbers under the charts are the relative energies with respect to Gly-Gly$^{\bullet+}$_O∴O.

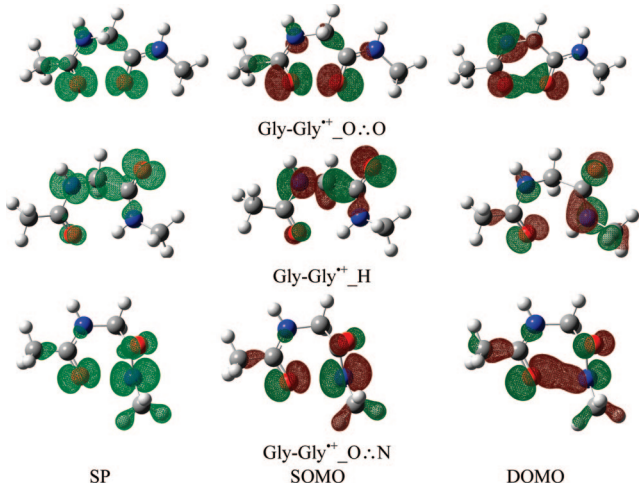

Figure 2. The plots of spin density surfaces (SP), singly occupied molecular orbitals (SOMO), and the second doubly molecular orbitals (HOMO-1) for the four representative isomers of Gly-Gly$^{\bullet+}$.

dipeptides are in the following order: Gly-X$^{\bullet+}$_H > Gly-X$^{\bullet+}$_O∴O > Gly-X$^{\bullet+}$_O∴N, which are different from Gly-Gly$^{\bullet+}$ with an order: Gly-Gly$^{\bullet+}$_O∴O > Gly-Gly$^{\bullet+}$_H > Gly-Gly$^{\bullet+}$_O∴N. More importantly, the stability of Gly-X$^{\bullet+}$_H, relative to Gly-X$^{\bullet+}$_O∴O, increases with the increase of the electron denoting ability of a side chain (Table 1).[60] This result further validates that formation of the O∴O bond is energetically more favorable than that of the O∴N bond, but the electron-donating property of the side-chain is more favorable to delocalization of the hole on the main chain backbone of dipeptide than to localization on the two close atoms (O/O or O/N).

Knowledge of the ionization potential of the various fragements in the protein environment is fundamental in the understanding of the electron-transfer processes in proteins. Therefore, the vertical ionization potentials for the main isomers of the dipeptide models were also calculated at the same level and given in Table 2. The vertical ionization potential is the difference in energy between a radical cation and its corresponding closed-shell isomer without change in structure (the latter has a more electron than the former). Interestingly, the vertical ionization potential of the O∴O bonded isomer is the lowest among all the isomers for the same dipeptide model as shown in Table 2. Clearly, the experiment fact that the electron hole in proteins can travel until it is trapped at a low ionization potential site has also suggested that the formation of O∴O bond favors the hole migration from a high ionization potential site to the O∴O bonded site.

3.3. Competitive Formation of O∴O 3e Bond versus Other S-contained 3e Bonds. Both of Cys and Met contain sulfuranyl groups, which present special behaviors during protein redox reactions. Therefore, single-electron oxidation of these two moieties in proteins has been extensively investigated involving sulfur-centered 3e bonds.[32,43,61−67] In this work, we selected the Gly-Cys and Gly-Met dipeptides as the target models to investigate the formation of the 2c-3e bonds after one-electron oxidation of them. Obviously, formation of the O∴O bonds competes with that of the 2c-3e bonds between >S$^{\bullet+}$ and other heteroatoms (O and N). For Gly-Cys$^{\bullet+}$, the O∴O bonded intermediate can be still emerged, while our calculations can not find existence of the O∴O bonds in Gly-Met$^{\bullet+}$. This is because the ionization energy of CH_3-S-CH_2- fragment in the side chain of Met is lower than that of $H-S-CH_2-$ fragment in Cys owing to the electron-donating property of methanyl group.

For Gly-Cys$^{\bullet+}$, the most stable conformer is an O∴S bonded isomer, named as Gly-Cys$^{\bullet+}$_O∴S$_1$, with the O∴S distance of 2.41 Å stabilized by an intramolecular O∴S bond and two weak H-bonds (N−H···N and C−H···O, Supporting Information, Figure S11). The TD-DFT calculated energy band for this O∴S bond is 3.12 eV, λ = 397.4 nm, which reflects that an electron transfers from the doubly occupied σ-orbital, DOMO, to the singly occupied σ*-orbital, SOMO, (see Supporting Information). These results fit well with the previous experimental[67,68] and calculated[42] values about the O∴S bonds. The O∴O bonded isomer, Gly-Cys$^{\bullet+}$_O∴O, is significantly higher in energy than Gly-Cys$^{\bullet+}$_O∴S$_1$ by 15.0 kcal/mol. This result indicates that formation of the O∴S bond is energetically more favorable than that of the O∴O bond for Gly-Cys$^{\bullet+}$.

For Gly-Met$^{\bullet+}$, there are no O∴O and O∴N bonded conformers. The lowest-energy isomer on the potential energy surface is an O∴S bonded structure, named as Gly-Met$^{\bullet+}$_O∴S$_1$. Here the distance of the O∴S bond is 2.42 Å and the spin densities mainly localize on the S-atom (0.74) and the close O-atom (0.23) (Supporting Information, Figure S12). This finding is in excellent agreement with previously reported results.[45,46,68] Besides, there is an intramolecular H-bond between another acyl O-atom and the amide H-atom with a length of 1.97 Å. Therefore, the O∴S bond and the intramolecular H-bond play important roles in stabilizing Gly-Met$^{\bullet+}$_O∴S$_1$. The second representative isomer is an N∴S bonded conformer, named as Gly-Met$^{\bullet+}$_S∴N$_1$ where a close S···N distance is 2.69 Å with the spin densities entirely lying on the S-atom (0.65) and the corresponding close N-atom (0.27). The S···N distance (2.69 Å) well consists with Hug's value (2.72 Å).[63] This agreement further validates that the DFT method is suitable to explore formation of the 2c-3e bond in proteins.

Mechanistically, when the presence of S-atom in the side chain of polypeptides, single-electron oxidation of proteins may be described as removing an electron from the S-atom, thus yielding a sulfur radical cation (>S$^{\bullet+}$). This sulfur radical easily provides a singly occupied lone pair orbital to form a new 2c-3e bond with doubly occupied lone pair of other heteroatoms (O or N) in its neighboring groups. These sulfur-center 3e bonds (O∴S and N∴S) play an important role not only in stabilizing proteins but also in promoting the electron hole migration in

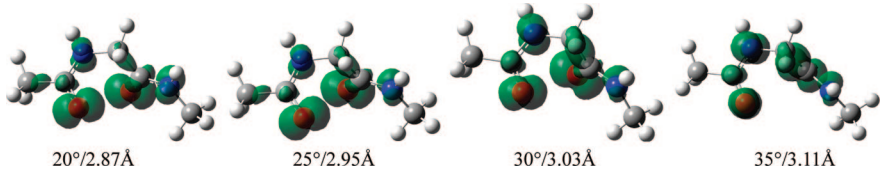

Figure 3. The dependence of the spin density distributions of Gly-Gly$^{\bullet+}$ on the dihedral NCCO (D_{NCCO}) obtained from the B3LYP/6-311+G* calculations. The first number under the picture is D_{NCCO} and the second is the O···O distance.

TABLE 1: The Relative Energies (in kcal/mol) of the Representative Isomers for Dipeptide Radical Cations

X	side chain (−R)	Gly-X$^{\bullet+}$_O∴O	Gly-X$^{\bullet+}$_O∴N	Gly-X$^{\bullet+}$_H
Gly	−H	0.0	3.3	2.2
Asp	$-CH_2COOH$	0.0	1.3	−0.3
Ala	$-CH_3$	0.0	4.6	−0.02
Pro	$-(CH_2)_3-$	0.0	5.4	−1.7
Arg	$-(CH_2)_3NH-$	0.0	1.8	−2.7
Val	$-CH(CH_3)_2$	0.0	1.1	−2.9

TABLE 2: The Vertical Ionization Potentials (in eV) for the Representative Isomers for the Dipeptide Radical Cations

X	side chain (−R)	Gly-X$^{\bullet+}$_O∴O	Gly-X$^{\bullet+}$_O∴N	Gly-X$^{\bullet+}$_H
Gly	−H	7.24	7.77	8.14
Asp	$-CH_2COOH$	6.90	7.37	7.92
Ala	$-CH_3$	7.13	7.41	7.84
Pro	$-(CH_2)_3-$	6.42	7.38	7.80
Arg	$-(CH_2)_3NH-$	9.27	9.56	9.92
Val	$-CH(CH_3)_2$	7.17	7.61	7.70

proteins as relay stations.[32,43,63,69] In this case, formation of the O∴O bonds competes with that of the O∴S bonds (or the N∴S bonds) and the latter is thermodynamically more favorable than the former.

3.4. Competitive Formations of O∴O versus O∴π Bonds for Aromatic Amino Acids. His, Phe, Tyr, and Trp are four aromatic amino acids among the 20 natural α-amino acids and may show some similar character when ionized. Similar to Gly-Gly$^{\bullet+}$, the O∴O bonded isomer can occur in Gly-Phe$^{\bullet+}$, named as Gly-Phe$^{\bullet+}$_O∴O, as shown in Figure 4. However, this O∴O bonded isomer is not the global minimum on potential energy surface but a local minimum. The most stable isomer, named as Gly-Phe$^{\bullet+}$_O∴π_1, is 11.1 kcal/mol below the Gly-Phe$^{\bullet+}$_O∴O. The salient structural characteristic for this isomer is a peptide O-atom close to the aromatic ring with the short distance of 2.35 Å between the O-atom and a C-atom of the aromatic ring (Figure 4). Besides, here a weak intramolecular H-bond is formed between one peptide O-atom and the other peptide H-atom with a H-bond length of 1.98 Å. The Mulliken spin density delocalizes mainly on the aromatic ring (0.60) and only partly on the close O-atom (0.29). The spin density surface also exhibits a consistent character with SOMO, an antibonding MO with an electron (Figure 5). It is noteworthy that a doubly

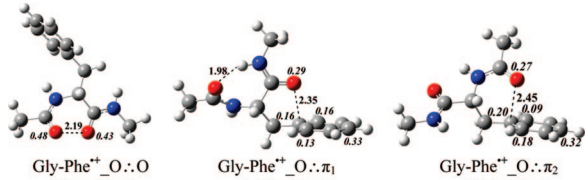

Figure 4. The representative isomers of Gly-Phe$^{\bullet+}$ predicted with the B3LYP/6-311+G* method. The selected bond distances are in angstroms; the italic numbers are the atomic spin densities; and the numbers under the charts are the corresponding energies with respect to the first isomer.

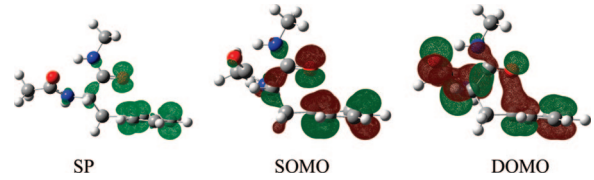

Figure 5. The plots of spin density surfaces (SP), singly occupied molecular orbitals (SOMO) and the corresponding doubly occupied molecular orbitals (DOMO) for Gly-Phe$^{\bullet+}$_O∴π_1, predicted with the B3LYP/6-311+G* method.

occupied MO (DOMO) describes a bonding interaction between the close acyl O-atom and the aromatic ring. In this case, combination of these two MOs yields a special 3e bond between the aromatic ring and the close O-atom, defined as the O∴π 3e bond. Therefore, two main stabilization factors, the O∴π bond and the intramolecular N−H···O H-bond, place Gly-Phe$^{\bullet+}$_O∴π_1 11.1 kcal/mol below Gly-Phe$^{\bullet+}$_O∴O. In contrast to Gly-Phe$^{\bullet+}$_O∴π_1, the last representative isomer, Gly-Phe$^{\bullet+}$_O∴π_2, also has an O∴π 3e bond with the other peptide O-atom approaching to the aromatic ring. In this case, Gly-Phe$^{\bullet+}$_O∴π_2 is 9.2 kcal/mol below Gly-Phe$^{\bullet+}$_O∴O and 1.9 kcal/mol above Gly-Phe$^{\bullet+}$_O∴π_1. The similar phenomena can be observed from the isomers of Gly-His$^{\bullet+}$ (Supporting Information, Figure S13).

However, for Gly-Tyr$^{\bullet+}$ and Gly-Trp$^{\bullet+}$, our calculations cannot find formation of the corresponding O∴O bonded isomers because their side-chains, phenol and indole, have low vertical ionization energies[70,71] and the electron hole (the unpaired electron) essentially resides on their aromatic rings. In this case, the aromatic ring with an electron hole is stabilized by forming an O∴π bond with the neighboring acyl O-atom. Therefore, the O∴π bonded conformers are formed for Gly-Tyr$^{\bullet+}$ and Gly-Trp$^{\bullet+}$ (Supporting Information, Figures S15 and S16). Similar to Gly-Phe$^{\bullet+}$, the most stable isomers are the O∴π bonded conformers. Actually, the ═O···π interaction has been also suggested to stabilize the protein structures in which the doubly occupied sp^2 hybrid orbital localized on the carbonyl O of the side-chain of amino acid residues interacts with the π^* antibonding orbital localized on the aromatic ring of the other residues.[26,27,72−75] Clearly, this coupling can provide a favorable structural basis for formation of the O∴π bond. At the same time, it can also favor energetically the stabilization of the electron hole by lowering the energies of the ionized products.

As seen in the above analyses, it is clear that formation of the O∴O bond is competitive with that of the O∴π bond when an aromatic ring is present in the side chain of the oligopeptide radical cation. For Gly-His$^{\bullet+}$ and Gly-Phe$^{\bullet+}$, formation of the O∴O bond is possible; nevertheless formation of the O∴π bonded isomers is thermodynamically more efficient than that of the O∴O bonded isomer. However, the O∴O bond cannot be formed in Gly-Tyr$^{\bullet+}$ and Gly-Trp$^{\bullet+}$. The most favorable conformers for these two dipeptides are the O∴π bonded isomers. This is because the side chains of Tyr and Try have low ionization energies[70,71] and formation of the O∴π bond plays an important role in stabilizing dipeptides. Furthermore,

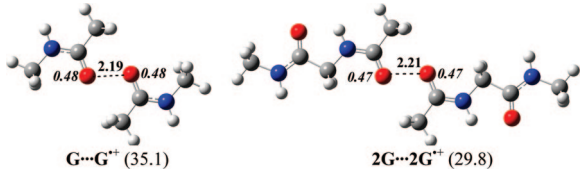

Figure 6. The geometries for O∴O bonded species between two main chains (G···G•+ and 2G···2G•+), predicted with the B3LYP/6-311+G* method. The selected bond distances are in angstroms; the italic numbers are the atomic spin densities; and the binding energies in parentheses are in kcal/mol.

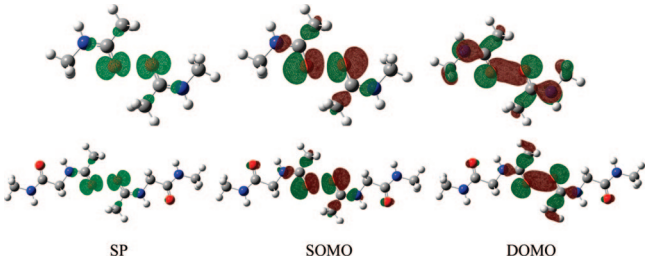

Figure 7. The plots of spin density surfaces (SP), singly occupied molecular orbitals (SOMO), and corresponding doubly occupied molecular orbitals (DOMO) for G···G•+ and 2G···2G•+.

the O∴π bonds may serve as the relay stations to favor the electron hole migration along polypeptide chains, implying the electron hole transport from the aromatic side chain to the peptide unit or vice-versa. Therefore, formation of the O∴π bonds may play an important role in assisting the electron hole migration along the peptide chains in proteins when the aromatic rings present in the side-chains of proteins.

3.5. Formation of the Interpeptide-Chain O∴O 3e Bonds in Proteins. To address the formation possibility of the O∴O bonds between two close main chains, two simple models, one containing a peptide bond unit (G) and the other containing two peptide bond units (2G), were considered. The binding modes in these two representative models (G···G•+ and 2G···2G•+) are shown in Figure 6 with the main parameters and the binding energies. For G···G•+, the closest O···O distance between two separated peptide units is only 2.19 Å and the unpaired electron essentially localizes on the two contacted O-atoms (0.48/0.48). The interaction between the singly occupied antibonding σ* MO (SOMO) and a doubly occupied bonding σ MO (DOMO) yields a 3e σ-bond between two O-atoms (Figure 7). The binding energy, defined by the difference between the energy of G···G•+ and the sum of the energies of the separate radical ionic (G•+) and G, is 35.1 kcal/mol (34.4 kcal/mol at MP2/6-311+G*//MP2/6-31+G* level). The similar properties can be found for a big model system, 2G···2G•+ (displayed in Figures 6 and 7). Besides, the similar O∴π bonds have also been formed between two different main chains.

These observations indicate that it is possible to form the O∴O bond between two close main chains during the protein redox processes. Clearly, formation of this kind of the O∴O 3e bond plays an important role not only in stabilizing the proteins but also in promoting the electron hole transport between two main chains via two proximal O-atoms of peptide units. That is, the O∴O bond between two proximal main chains of proteins may serve as a relay station to help electron hole transport from one main chain to the next.

3.6. Molecular Dynamics Simulations on 3e Bonds. ***3.6.1. Dynamics Stability of 3e Bonds.*** AIMD simulations allow time-dependent properties of the molecules to be explored. Figure 8A shows the change of radial distribution functions (RDF) for the O···O distance at a time period of 20.0 fs for 1.0 ps beginning with the optimized geometry of Gly-Gly•+_O∴O. The change of the O···O distance lies in the range 2.10∼2.60 Å, indicating that two carbonyl O are always linked by a bond. Besides, to confirm the stabilization of Gly-Gly•+_O∴O, a further AIMD simulation was carried out for another 5.0 ps with a time step of 1.0 fs. The average mean square displacement (AMSD) for the O-atoms and RDF for the O···O distance ($g_{OO}(r)$) are displayed in Figure 9. It is clear from the plot that the system arrives at an equilibrium state because the time dependence of the MSD for the O-atoms is nearly linear. More interestingly, RDF (g(r)) reveals that the O···O distance falls always in the range of 2.00∼3.00 Å during this simulation process, which implies that two O-atoms is kept linked by a 3e bond. This observation further corroborates that Gly-Gly•+_O∴O is the lowest-energy isomer on the global potential energy surface at 300 K. For all the other dipeptide radical cations, the corresponding lowest-energy isomers on the potential energy surfaces were also certified by this method.

As far as Gly-Ala•+ dipeptide is concerned, AIMD simulations were carried out on the basis of the optimized structure of Gly-Ala•+_O∴O for 6.0 ns. Figure 8B shows the change of RDF for the O···O distance with a time period of 20.0 fs for the first 1.0 ps. Inspection of Figure 8(B) shows that the highest peaks lie in the range of 2.20∼3.00 Å for the O···O distance and the corresponding time is in the range of 0∼155.2 fs. This observation also indicates that the time is long enough for ET from a peptide unit to the next. After 155.2 fs, the O···O distance is longer than 3.00 Å, implying that the O∴O bond is destroyed. Interestingly, the conformation of Gly-Ala•+ varies with an elongation of the O···O distance (Figure 8(B)) and a rotation of dihedral angle $N_4C_5C_6O_2$ (Scheme 2), and then eventually reaches to the lowest-energy conformation, Gly-Ala•+_H. In the following 5.0 ps simulation, the plot of the RDF for the H-bond (O···H) indicates that the O···H distance lies mainly in the range of 1.50∼2.50 Å (Figure 10 B), which further substantiates that Gly-Ala•+_H is the lowest minimum on the potential energy surface at 300.0 K. The similar processes can be found for Gly-Val•+, Gly-Arg•+, and Gly-Asp•+, starting from the optimized structures of their corresponding O∴O bonded isomers.

3.6.2. Hole Migration along the Peptide Chain. In order to explore the migration processes of electron hole along the peptide chains, the AIMD simulations were carried out on a series of the polypeptide radical cations at 300 and 1000 K.[57] Our calculational results indicate that it is difficult to simulate a continuous formation of O∴O bonds along all the polypeptides at 300 K. This is because the systems are at the quiescent OFF state and it is very slow to change conformation to form O∴O bonds along the peptide chains at 300 K. Therefore, the further AIMD simulations were carried out at 1000 K.[57] Here, the simulation of 3Gly•+ at 1000 K is taken as an example. Snapshots of the time evolution of structures of 3Gly•+ radical cation are drawn in Figure 11. The RSDs for the two O···O distances of 3Gly•+ during the first 1500 fs simulation and the time evolution of the formation of O∴O bonds (OO_1 and OO_2) are shown in Figure 12. The beginning structure of 3Gly•+ are obtained after a 6.0 ps simulation at 300 K, as displayed in Figure 11. For the first 41 fs, the OO_2 distance shortens slowly with elongating the OO_1 distance. The OO_2 distance begins to be less than 3.00 Å at 19 fs and the OO_2 distance is 2.83 Å at 41 fs as shown in Figure 11. After 41 fs, the OO_2 distance starts to lengthen and the OO_1 distance shortens. At 79 fs, the OO_2 distance increases to 3.00 Å. That is, the length of OO_2 is less

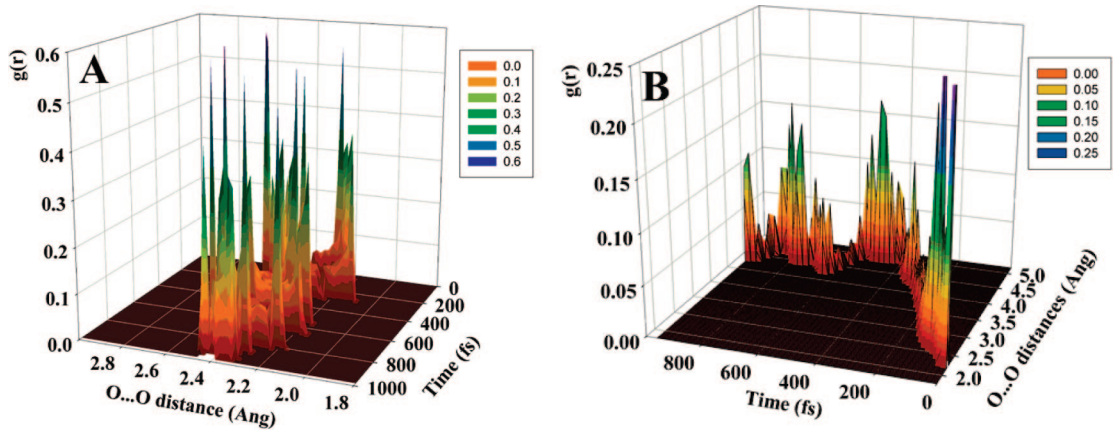

Figure 8. The changes of radial distribution functions (RDF) with time at a time period of 20.0 fs for 1.0 ps starting from the optimized geometries of Gly-Gly$^{\cdot+}$_ O∴O (A) and Gly-Ala$^{\cdot+}$_ O∴O (B).

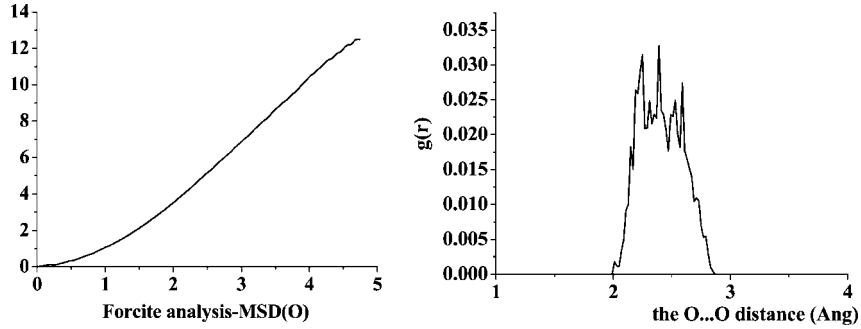

Figure 9. The AMSD and RDF for the Gly-Gly$^{\bullet+}$_O∴O conformer for 1.0∼6.0 ps.

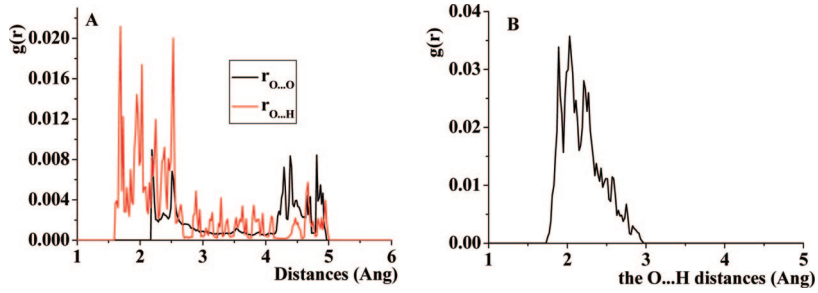

Figure 10. The RDF for the Gly-Ala$^{\bullet+}$ cation radical starting from the optimized geometry of Gly-Ala$^{\bullet+}$_t. (A) displays the plot of RDF for the first 1.0 ps and (B) does for the following 5.0 ps.

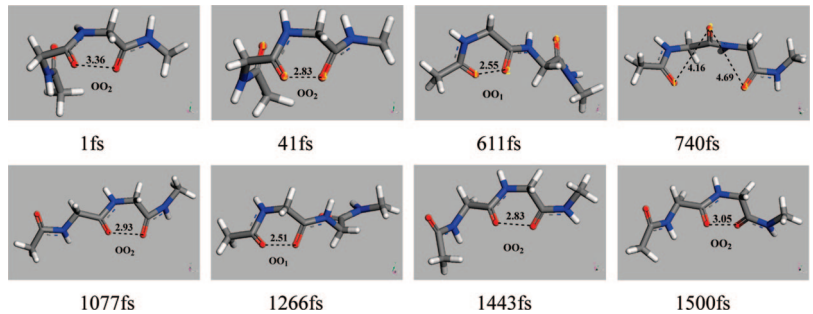

Figure 11. Several snapshots of representative configurations of ab initio MD simulations of 3Gly$^{\bullet+}$. The number under the picture is the simulation time.

than 3.00 Å in the time range of 19∼79 fs and the two O-atoms are linked by a 3e bond during this process. As the rotation of framework of 3Gly$^{\bullet+}$, the OO_1 distance reduces slowly and steadily. After 542 fs, the length of OO_1 begins to be less than 3.00 Å, and it reaches to the minimum of 2.55 Å at 611 fs (Figure 11). After 611 fs, the OO_1 distance starts stretching with shortening the OO_2 distance, and finally elongates to 3.00 Å at 650 fs. This indicates that the O_1 and O_2 atoms are linked by a 3e bond from 542 to 650 fs. In the following 483 fs, no OO 3e bonds are formed in the system. Then from 1033 to 1112 fs,

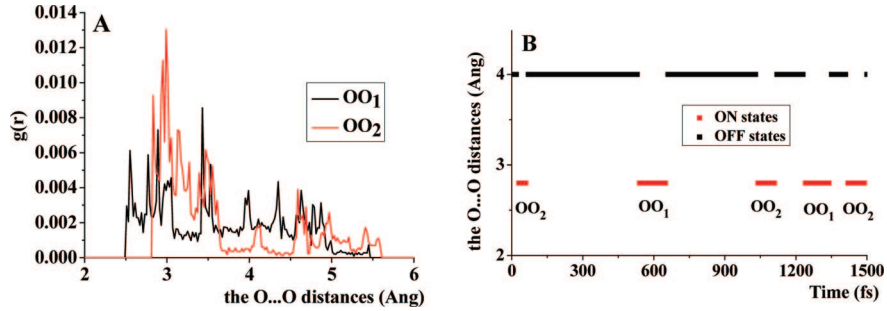

Figure 12. (A) The radial distribution functions (RDF) for the two O···O distances of $3Gly^{\bullet+}$ during the first 1500 fs simulation. (B) The symbol of the change of ON/OFF states for $3Gly^{\bullet+}$ for the first 1500 fs simulation. The below red lines (ON state) note that the distance of a two neighboring O-atoms of $3Gly^{\bullet+}$ is less than 3.00 Å and the above bold lines (OFF state) denote that no two O-atoms lies less than 3.00 Å.

the 3e bond is also formed between the O_2 and O_3 atoms. Thus, the OO_1 and OO_2 3e bonds are alternately formed during this AIMD simulation progress, as shown in Figures 11 and 12. These simulation results further validate that it is possible to form the O∴O bonded species during electron hole migration process in protein and these O∴O bonds may act as relay stations to favor the electron hole transport along the peptide chain. At least in the case of polypeptide, our models were able to perform the task, providing information not accessible by means of experimental models. Besides, for a big size polypeptide radical cation ($4Gly^{\bullet+}$ or $6Gly^{\bullet+}$), the O∴O bond can also be formed between the random two neighboring peptide units at 1000 K,[57] but it is stochastic rather than coherent for the formation of the O∴O bonds along the peptide chains. This may be explained by the hopping mechanism of the electron hole transfer in proteins.[12−19] Much more extensive simulations are underway to test this possibility.

Discussion and Conclusion

Our theoretical analyses reveal a possibility to form a series of 3e bonds (O∴O and O∴π) in the oligopeptide radical cations and the formations of these 3e bonds may help charge transport along the peptide. Evidently, the stability of the O∴O bonded species is strongly dependent on the component of the oligopeptide radical cations. In most cases, formation of the O∴O bonded isomers is not thermodynamically favorable and the O∴O bonded isomers are only the local minima on the potential energy surfaces. Although existence of the O∴O bonds is only instantaneous during the protein redox processes, it plays an important role in assisting the electron hole transport along the peptide chains. The finding of the O∴O bonds in the oligopeptides may explain the charge transfer between the proximal peptide units in proteins,[20,22] supporting peptide chains as conduction wires. Besides, when a sulfur atom presents in the side chains, formation of the O∴O bonds competes with that of the S-centered 3e bonds including the O∴S and N∴S. As mentioned above, it is impossible to form the O∴O bond in $Gly\text{-}Met^{\bullet+}$ and the most favorable isomer is one with an O∴S bond, $Gly\text{-}Met^{\bullet+}\_O\therefore S_1$. However, when an aromatic ring presents in the side chains, formation of the O∴O bonds is competitive with that of the O∴π bonds and the latter is thermodynamically more favorable than the former.

Further, the O∴O bond can be encountered in all dipeptide radical cations except for $Gly\text{-}Trp^{\bullet+}$, $Gly\text{-}Tyr^{\bullet+}$, and $Gly\text{-}Met^{\bullet+}$. This may be understood as a result of that the vertical ionization energies of the side chains of Trp, Tyr, and Met (3-methylindole, 4-methylphenol, and methylthioethane) are the lowest among all the side chains of 20 natural amino acids (Supporting Information, Table S3), being 7.12, 7.81, and 8.44 ev, respectively. This implies that oxidation of Trp, Tyr, or Met causes removal of an electron from their side chains, thus being impossible to form the O∴O bond between two proximal peptide units in their dipeptide radical cations. However, the vertical ionization energies of the side chains of other amino acids are high[22] and the O∴O bonds can be formed in $Gly\text{-}X^{\bullet+}$. Therefore, the high ionization energies for the side chains of amino acids favor formation of the O∴O bonds between two approximal peptide units in the dipeptide radical cations.

Besides, the O∴O bond can be encountered between two peptide units in different main chains. The short O···O distance of 2.19 Å and the big binding energy of 35.1 kcal/mol for G···G strongly support formation of the O∴O bond between two proximal main chains in proteins during the electron hole migration processes.

Therefore, we infer that formation of a series of 3e bonds, including the O∴O, O∴S, N∴S, and O∴π bonds, may play an important role in assisting the electron hole migration along the peptide chains or between chains in proteins serving as intermediates or relay stations. Schlag proposed that the charge transfer can occur between two neighboring peptide units in the oligopeptides by two steps.[20] One step is to rotate two carbonyl groups of adjacent amino acids, causing the distance between two carbonyl O-atoms being less than 3.00 Å, and the second step is the quick charge transfer without energy barrier. Therefore, formation of the O∴O bonds between the two adjacent peptide units bears responsibility for the charge transfer from one peptide to the next. Our AIMD simulations of the polypeptide radical cations also support this conclusion. Besides, the O∴O bonds are also formed between peptide units in two proximal main chains and act as relay stations for the electron hole migration from one main chain to the next. When Met or Cys presents in main chains of proteins, the O∴S or N∴S bond does as a relay station to assist the electron hole transport from the adjacent peptide unit to the S-group of the side chain. Similarly, when the aromatic amino acids, including His, Phe, Tyr, and Trp, are present in proteins, formation of the O∴π bonds between the aromatic ring and an O-atom of approximal peptide unit is thermodynamically favorable during the electron hole migration process in proteins, thus promoting the protein electron hole transport.

In summary, our findings regarding a series of 3e bonds in proteins may significantly help to understand the conduction property of the peptides and also provide a guidance for further theoretical investigations on the protein charge transfer processes through the electron hole migration mechanism. Thus, additional studies aiming at extending the size and complexity of the systems considered in the present work are in progress.

Acknowledgment. We sincerely thank the referees for their extremely helpful comments. This work is supported by NSFC (20633060, 20573063), NCET, sdNSF(Z2003B01), and the Virt Laboratory for Comput Chem of CNIC-CAS. Calculations were performed on the HPCC at SDU and SCC of CNIC-CAS.

Supporting Information Available: The complete citation for ref 50 as well as the calculated molecular geometries, spin densities, orbital characters, relevant energetics, ultraviolet spectra, and Cartesian coordinates for all dipeptide radical cations and correlations among several quantities. This material is available free of charge via the Internet at http://pubs.acs.org.

References and Notes

(1) Page, C. C.; Moser, C. C.; Chen, X. X.; Dutton, P. L. *Nature* **1999**, *402*, 47–52.

(2) Photochemistry and Radiation Chemistry, Complementary Methods for the Study of Electron-Transfer. *ACS Advances in Chemistry Series 254*; Wishart, J. F., Nocera, D. G., Eds.; American Chemical Society: Washington, DC, 1998.

(3) Prytkova, T. R.; Kurnikov, I. V.; Beratan, D. N. *Science* **2007**, *315*, 622–625.

(4) Yang, H.; Luo, G. B.; Karnchanaphanurach, P.; Louie, T. M.; Rech, I.; Cova, S.; Xun, L. Y.; Xie, X. S. *Science* **2003**, *302*, 262–266.

(5) Osyczka, A.; Moser, C. C.; Daldal, F.; Dutton, P. L. *Nature* **2004**, *427*, 607–612.

(6) Belevich, I.; Verkhovsky, M. I.; Wikstrom, M. *Nature* **2006**, *440*, 829–832.

(7) Bauer, A.; Westkamper, F.; Grimme, S.; Bach, T. *Nature* **2005**, *436*, 1139–1140.

(8) Wasielewski, M. R. Distance dependencies of electron transfer reactions. In *Photoinduced Electron Transfer*; Fox, M. A., Chanon, M., Eds.; Elsevier: Amsterdam, 1988; Vol. A.

(9) Pujols-Ayala, I.; Sacksteder, C. A.; Barry, B. A. *J. Am. Chem. Soc.* **2003**, *125*, 7536–7538.

(10) Shin, Y. G.; Newton, M. D.; Isied, S. S. *J. Am. Chem. Soc.* **2003**, *125*, 3722–3732.

(11) Malak, R. A.; Gao, Z.; Wishart, J. F.; Isied, S. S. *J. Am. Chem. Soc.* **2004**, *126*, 13888–13889.

(12) Weinkauf, R.; Aicher, P.; Wesley, G.; Grotemeyer, J.; Schlag, E. W. *J. Phys. Chem.* **1994**, *98*, 8381–8391.

(13) Weinkauf, R.; Schanen, P.; Yang, D.; Soukara, S.; Schlag, E. W. *J. Phys. Chem.* **1995**, *99*, 11255–11265.

(14) Weinkauf, R.; Schanen, P.; Metsala, A.; Schlag, E. W.; Burgle, M.; Kessler, H. *J. Phys. Chem.* **1996**, *100*, 18567–18585.

(15) Remacle, F.; Levine, R. D.; Schlag, E. W.; Weinkauf, R. *J. Phys. Chem.* **1999**, *103*, 10143–10158.

(16) Schlag, E. W.; Sheu, S. Y.; Yang, D. Y.; Selzle, H. L.; Lin, S. H. *J. Phys. Chem. B* **2000**, *104*, 7790–7794.

(17) Petrov, E. G.; Shevchenko, Ye V.; Teslenko, V. I.; May, V. J. *Chem. Phys.* **2001**, *115*, 7107–7122.

(18) Morita, T.; Kimura, S. J. *Am. Chem. Soc.* **2003**, *125*, 8732–8733.

(19) Giese, B.; Napp, M.; Jacques, O.; Boudebous, H.; Taylor, A. M.; Wirz, J. *Angew. Chem., Int. Ed.* **2005**, *44*, 4073–4075.

(20) Schlag, E. W.; Sheu, S. Y.; Yang, D. Y.; Selzle, H. L.; Lin, S. H. *Proc. Natl. Acad. Sci. U.S.A.* **2000**, *97*, 1068–1072.

(21) Woutersen, S.; Mu, Y.; Stock, G.; Hamm, P. *Proc. Natl. Acad. Sci. U.S.A.* **2001**, *98*, 11254–11258.

(22) Schlag, E. W.; Sheu, S. Y.; Yang, D. Y.; Selzle, H. L.; Lin, S. H. *Angew. Chem., Int. Ed.* **2007**, *46*, 3196–3210.

(23) DiLabio, G. A.; Ingold, K. U. A. *J. Am. Chem. Soc.* **2005**, *127*, 6693–6699.

(24) DiLabio, G. A.; Johnson, E. R. *J. Am. Chem. Soc.* **2007**, *129*, 6199–6203.

(25) Chen, X.; Bu, Y. *J. Am. Chem. Soc.* **2007**, *129*, 9713–9720.

(26) Jain, A.; Purohit, C. S.; Verma, S.; Sankararamakrishnan, R. *J. Phys. Chem. B* **2007**, *111*, 8680–8683.

(27) Egli, M.; Sarkhel, S. *Acc. Chem. Res.* **2007**, *40*, 197–205.

(28) Burley, S. K.; Petsko, G. A. *Science* **1985**, *229*, 23–28.

(29) Dougherty, D. A. *Science* **1996**, *271*, 163–168.

(30) Quinonero, D.; Garau, C.; Rotger, C.; Frontera, A.; Ballester, P.; Costa, A.; Deya, P. M. *Angew. Chem., Int. Ed.* **2002**, *41*, 3389–3392.

(31) de Rege, P. J.; Williams, S. A.; Therien, M. J. *Science* **1995**, *269*, 1409–1413.

(32) Schöneich, C.; Pogocki, D.; Hug, G. L.; Bobrowski, K. *J. Am. Chem. Soc.* **2003**, *125*, 13700–13713.

(33) Chatgilialoglu, C.; Asmus, K.-D. *Sulfur-Centered Reactive Intermediates in Chemistry and Biology*; Plenum Press: New York, 1991; pp 389−399.

(34) Clark, T. *J. Am. Chem. Soc.* **1988**, *110*, 1672–1678.

(35) Braida, B.; Hazebroucq, S.; Hiberty, P. C. *J. Am. Chem. Soc.* **2002**, *124*, 2371–2378.

(36) Braida, B.; Thogersen, L.; Wu, W.; Hiberty, P. C. *J. Am. Chem. Soc.* **2002**, *124*, 11781–11790.

(37) Pauling, L. *J. Am. Chem. Soc.* **1931**, *53*, 3225–3237.

(38) James, M. A.; McKee, M. L.; Illies, A. J. *J. Am. Chem. Soc.* **1996**, *118*, 7836–7842.

(39) Gauduel, Y.; Gelabert, H.; Guilloud, F. J. *J. Am. Chem. Soc.* **2000**, *122*, 5082–5091.

(40) Goez, M.; Rozwadowski, J.; Marciniak, B. *Angew. Chem., Int. Ed. Engl.* **1998**, *37*, 628–630.

(41) Schöneich, C.; Pogocki, D.; Hug, G. L.; Bobrowski, K. *J. Am. Chem. Soc.* **2003**, *125*, 13700–13713.

(42) Pogocki, D.; Serdiuk, K.; Schöneich, C. *J. Phys. Chem. A* **2003**, *107*, 7032–7042.

(43) Bobrowski, K.; Hug, G. L.; Pogocki, D.; Marciniak, B.; Schöneich, C. *J. Am. Chem. Soc.* **2007**, *129*, 9236–9245.

(44) Schöneich, C. *Arch. Biochem. Biophys.* **2002**, *397*, 370–376.

(45) Schöneich, C. *Biochim. Biophys. Acta* **2005**, *1703*, 111–119.

(46) Rauk, A.; Armstrong, D. A.; Fairlie, D. P. *J. Am. Chem. Soc.* **2000**, *122*, 9761–9767.

(47) In this work, the amino acids will be represented by their three-letter abbreviations: Gly for glycine, Ala for alanine, Val for valine, Asp for asparagine, Cys for cysteine, Met for methionine, His for histidine, Phe for phenylalanine, Try for tyrosine, and Trp for tryptophan.

(48) Boys, S. F.; Benardi, F. *Mol. Phys.* **1970**, *19*, 553–566.

(49) Rappe, A. K.; Bernstein, E. R. *J. Phys. Chem. A* **2000**, *104*, 6117–6128.

(50) Frisch, M. J. *et al. Gaussian 03*, revision C.02; Gaussian, Inc.: Wallingford, CT, 2004.

(51) (a) Becke, A. D. *J. Chem. Phys.* **1993**, *98*, 5648–5652. (b) Lee, C.; Yang, W.; Parr, R. G. *Phys. Rev. B* **1988**, *37*, 785–789.

(52) (a) McLean, A. D.; Chandler, G. S. *J. Chem. Phys.* **1980**, *72*, 5639–5648. (b) Krishnan, R.; Binkley, J. S.; Seeger, R.; Pople, J. A. *J. Chem. Phys.* **1980**, *72*, 650–654. (c) Clark, T.; Chandrasekhar, J.; Spitznagel, G. W.; Schleyer, P. v. R *J. Comput. Chem.* **1983**, *4*, 294–301. (d) Frisch, M. J.; Pople, J. A.; Binkley, J. S. *J. Chem. Phys.* **1984**, *80*, 3265–3269.

(53) Kendall, R. A.; Dunning, T. H.; Harrison, R. J. *J. Chem. Phys.* **1992**, *96*, 6796–6806.

(54) Casida, M. E.; Jamorski, C.; Casida, K. C.; Salahub, D. R. *J. Chem. Phys.* **1998**, *108*, 4439–4449.

(55) Delley, B. J. *Chem. Phys.* **1990**, *92*, 508–517.

(56) *Cerius2*; BIOSYM/Molecular Simulations: San Diego, CA, 1996.

(57) In native charge-transfer systems an electron is transported between donor and acceptor through large peptides and the electron migration is driven by electromotive potential between donor and acceptor. In this work, only the electron transfer bridges−polypeptide cations without additional donor and acceptor units attached were investigated and "at 1000 K" are to add a voltage (0.085 eV) in the systems (ref 20).

(58) The Mulliken spin density analysis indicates that the spin density mainly distributes on the two trans carbonyl O-atoms of the peptide bonds (0.64 versus 0.25) for Gly-Gly$^{\bullet+}$_H_2. Gly-Gly$^{\bullet+}$_H_2 mounts only a lower barrier high (1.0 kcal/mol) to yield Gly-Gly$^{\bullet+}$_O∴O (Supporting Information, Figure S5) and the Gly-X$^{\bullet+}$_H_2 conformer can not come into being in all other dipeptide radical cation if there are no other stabilization factors, such as, hydrogen bonds and 3e bonds.

(59) The plot of spin density surface is in excellent agreement with that of SOMO (Figure 2), which is antibonding between the close O and N atoms. Besides, it is clear that HOMO-1 (here named as DOMO) of Gly-Gly$^{\bullet+}$_O∴N is a bonding MO between these two close atoms. Therefore, there is a 2c-3e bond between the close O and N atoms arising from the interaction between the SOMO and the DOMO.

(60) It is worth noting that there is an especial example, Gly-Asp$^{\bullet+}$_H, whose relative energy (−0.3 kcal/mol) is bigger than that of Gly-Ala$^{\bullet+}$_H (−0.02 kcal/mol). However, the ability of electron-denoting of−CH_3COOH in the side chain of Asp is weak relative to−CH_3 in the side chain of Ala. One of the plausible reasons is that the spin densities delocalize not only over the main chain but also on the carbonyl O-atom of−CH_3COOH in Gly-Asp$^{\bullet+}$_H (Supporting Information, Figure S8), which well disperses the positive charge compared to Gly-Ala$^{\bullet+}$_H and increases the stability.

(61) Gannett, P. M.; Garrett, C.; Lawson, T.; Toth, B. *Food Chem. Toxicol.* **1991**, *29*, 49–56.

(62) Hong, J.; Schöneich, C. *Free Radical Biol. Med.* **2001**, *31*, 1432–1441.

(63) Bobrowski, K.; Hug, G. L.; Pogocki, D.; Marciniak, B.; Schöneich, C. *J. Phys. Chem. B* **2007**, *111*, 9608–9620.

(64) Bobrowski, K.; Hug, G. L.; Marciniak, B.; Schöneich, C.; Wioeniowski, P. *Res. Chem. Intermed.* **1999**, *25*, 285–297.

(65) Bobrowski, K.; Hug, G. L.; Marciniak, B.; Miller, B. L.; Schöneich, C. *J. Am. Chem. Soc.* **1997**, *119*, 8000–8011.

(66) Asmus, K.-D.; Göbl, M.; Hiller, K.-O.; Mahling, S.; Mönig, J. *J. Chem. Soc., Perkin Trans.* **1985**, *8*, 641–646.

(67) Steffen, L. K.; Glass, R. S.; Sabahi, M.; Wilson, G. S.; Schoeneich, C.; Mahling, S.; Asmus, K. D. *J. Am. Chem. Soc.* **1991**, *113*, 2141–2145.

(68) Schoneich, C.; Pogocki, D.; Wisniowski, P.; Hug, G. L.; Bobrowski, K. *J. Am. Chem. Soc.* **2000**, *122*, 10224–10225.

(69) Glass, R. S. Neighboring group participation: General principles and application to sulfur-centered reactive species. In *Sulfur-Centered Reactive Intermediates in Chemistry and Biology*; Chatgilialoglu, C., Asmus, K.-D., Eds.; Plenum Press: New York, 1990; Vol. 97, pp 213−226.

(70) Bagheri-Majdi, E.; Ke, Y.; Orlova, G.; Chu, I. K.; Hopkinson, A. C.; Siu, K. W. M. *J. Phys. Chem. B.* **2004**, *108*, 11170–11181.

(71) It is well known that Trp and Tyr are easily oxidized in the processes of the protein redox reactions because both have the lowest ionization energies (IEs) among the natural α-amino acids. Their lowest IEs come from the special characters of their side chains, indole moiety in Trp and phenol moiety in Tyr. Our calculations indicate that the vertical IEs of 3-methylindole and 4-methylphenol are 7.40 and 7.96 eV, respectively, which agree well with previously results (ref 65). For the side chains of His and Phe, the vertical IEs of 2-methylimidazole and toluene are 8.55 and 9.00 eV, respectively, which are bigger than these of 3-methylindole and 2-methylphenol.

(72) Meyer, E. A.; Castellano, R. K.; Diederich, F. *Angew. Chem., Int. Ed.* **2003**, *42*, 1210–1250.

(73) Qian, X.; Xu, X.; Li, Z.; Frontera, A. *Chem. Phys. Lett.* **2003**, *372*, 489–496.

(74) Lovell, S.; Davis, I.; Arendall, W., III.; De Bakker, P.; Word, J.; Prisant, M.; Richardson, J.; Richardson, D. *Proteins: Struct., Funct., Genet.* **2003**, *50*, 437–450.

(75) Gung, B. W.; Zou, Y.; Xu, Z.; Amicangelo, J. C.; Irwin, D. G.; Ma, S.; Zhou, H.-C. *J. Org. Chem.* **2008**, *73*, 689–693.

JP805910X